Influence of surface functionalities on Li-ion intercalation performance of carbon cloth.

*Edgar Ventosa[1], Wei Xia[2], Stefan Klink[1], Fabio La Mantia[3], Martin Muhler[2], Wolfgang Schuhmann[*1]*

[1] Analytische Chemie – Elektoanalytik und Sensorik,

[2] Laboratory of Industrial Chemistry,

[3] Centre for Electrochemical Sciences ;

Ruhr-Universität Bochum, Universitätsstr. 150, D-44780 Bochum, Germany

***corresponding author: wolfgang.schuhmann@rub.de**

ABSTRACT.

Commercial carbon cloth made of PAN-based carbon fibres was used as free-standing anode for lithium intercalation. The role of surface functionalities on the irreversible specific charge and the reversible specific charge during the intercalation and de-intercalation of lithium ion into carbon cloth has been investigated. For this purpose, oxygenated groups have been introduced by nitric acid vapour treatment and, then, gradually removed by thermal treatments at different temperatures in helium or hydrogen atmosphere as has been confirmed by XPS. Clear correlation between oxygen amount and irreversible specific charge has been found. Three irreversible processes have been distinguished during the first negative-going sweep: reduction of oxygenated group, solid electrolyte interface (SEI) formation and exfoliation, although the latter one was only observed in samples with lower surface oxygen concentration than 4 %. As for the reversible process, increased specific charge upon increasing amount of oxygenated groups was also observed. However, the main improvement was seen above 1.5 V.

1. INTRODUCTION.

The power source for portable electronic devices such as laptops and mobile phones is currently dominated by lithium ion batteries, which are also candidates to power hybrid electric vehicles due to their high energy density {Tarascon 2001 #93}{Tarascon 2010 #267}{Bruce 2008 #14}[1-3]. Carbonaceous materials are the most common anodes and, therefore, a great effort has been devoted to gain a better understanding of the Li-ion intercalation process into these materials {Fong 1990 #184}{ZHENG 1995 #270}{DAHN 1995 #257} [4-6]. Under the standard operational conditions of graphite anodes, the electrolyte is thermodynamically not stable, and tends to be reduced. The products of its reduction form a film kwon as solid electrolyte interface (SEI) on the surface of the anode {Winter 1998 #99}{Aurbach 1994 #250}{Aurbach 1995 #251}[7-9]. This layer allows lithium ion diffusion and it is electrically insulating, which avoid further reduction of the electrolyte. On the one hand, the SEI formation is a necessary process since it acts as passivation layer which prevents electrode degradation upon cycling; on the other hand, the formation of the SEI contributes to the irreversible specific charge during the first cycle. The complexity and importance of the phenomena involved in the SEI formation has pushed the research to investigate deeply {Jeong 2001 #260}{Aurbach 1999 #249}{Novak 2005 #264} [10-12].

The irreversible process depends on properties such as morphology or composition of the resulting SEI layer which, in turn, rely on the electrolyte, the conditions of the film synthesis and the surface properties of the electrode {Larcher 1999 #262}{Spahr 2002 #265} [13-14]. The surface functionalities are among those many parameters that have been studied. However, there is still no agreement on whether the presence of surface functionalities influences the irreversible specific charge {Spahr 2003

#266} [15] or not {Beguin 2005 #198} [16]. Gaining more insight into the influence of this parameter is needed, especially since carbon nanotubes (CNT) have been proposed as active material in anodes {Gao 1999 #259}{Chen 2008 #255}{Landi 2008 #193}{Shimoda 2002 #175} [17-20]. The removal of impurities, metallic catalyst or amorphous carbon from commercial CNT as well as the improvement of dispersibility for electrode preparation demand the pre-treatment of CNT, which can introduce different modifications on its structure such as creating defects, opening of the ends or reducing the length {AJAYAN 1993 #252}{Klein 2008 #261}{Bitter 2010 #254} [21-23]. Consequently, it is difficult to distinguish the influence of each individual modification not only on the irreversible specific charge but also on the reversible specific charge.

Carbon cloth can be used as free standing electrode without binder, conductive additive and current collector {Beguin 2005 #198}{Beguin 2004 #243} [16,24]. The raw material can be easily subjected to different type of treatments and, then, investigated. The electrode morphology remains unchanged for sample subjected to a variety of treatments. It was therefore chosen as model material to study the influence of surface groups on the electrochemical performances of carbonaceous materials.

Herein, the influence of surface functionalities on the lithium ion intercalation performance of carbon cloth has been assessed. Samples containing different amounts and types of oxygenated surface groups have been prepared by oxidative and thermal treatments. The lithium ion deintercalation – intercalation process of all samples was evaluated and the main features of this process was correlated to the modification introduced onto the surface

2. EXPERIMANTAL SECTION

Sample preparation Carbon cloth (without additional surface treatment after production) was purchased from ETEK (NJ, USA). The carbon cloth was made of PAN-based carbon fibres (diameter about 6 μm). Different treatments were performed on the carbon cloth as shown in Figure 1. (1) As-received carbon cloth was treated at 800°C in flowing hydrogen for 2 h to remove surface impurities like polyaromatics; (2) As-received carbon cloth was treated in nitric acid vapour at 200°C for 24 h, 72 h or 144 h to create oxygen-containing functional groups {Xia 2009 #139} [25]. These samples are referred to as O-24h, O-72h and O-144h carbon cloth, respectively; (3) The sample O-24h was treated in flowing helium or hydrogen for 2 h at different temperatures, namely 300°C, 600°C and 800°C {Kundu 2008 #145} [26]. The obtained samples are referred to as O-24h-300He, O-24h-600He, O-24h-800He, O-24h-300H_2, O-24h-600H_2 and O-24h-800H_2, respectively. The obtained carbon cloth samples were used as free-standing electrode for Li intercalation.

Characterizations XPS measurements were carried out in an ultrahigh vacuum (UHV) setup equipped with a high-resolution Gammadata- cienta SES 2002 analyzer. A monochromatic Al Kα X-ray source (1486.6 eV; anode operating at 14 kV and 55 mA) was used as incident radiation. The base pressure in the measurement chamber was around 2×10^{-10} mbar. XP spectra were recorded in the fixed transmission mode. The analyzer slit width was set to 0.3 mm and a pass energy of 200 eV was chosen, resulting in an overall energy resolution better than 0.5 eV. Charging effects were compensated by applying a flood gun. The binding energies were calibrated based on the graphite C 1s peak at 284.5 eV. Prior to individual elemental scans, a survey scan was taken for all the samples to find out all of the elements present. The CASA XPS program with a Gaussian-Lorentzian mix function and Shirley background subtraction was employed to deconvolute the XP spectra. The peak positions were reproducible along with the fixed

Lorentz to Gaussian ratio and FWHM. Care was taken that all the fitting results are self-consistent, so that the corresponding deconvoluted peaks can be compared quantitatively.

Electrochemistry. Electrochemical studies were carried out under argon atmosphere in a three electrode setup where metallic lithium sheet was used as both counter and reference electrodes and a piece of carbon cloth of ca 5 mg as working electrode. A solution which consists of 1 M $LiClO_4$ in a 1:1 (volume) mixture of ethylene carbonate (EC) and dimethyl carbonate (DMC) from Sigma-Aldrich was used as electrolyte. A microAutolab type III was utilized to perform galvanostatic chronopotentiometry in the voltage range from 3.00 to 0.01 V. All potential values in this work are given versus Li/Li^+. A specific current of 100 mAg^{-1} was applied during the first cycles to study the irreversible processes since a better visualization of different peaks were observed at high rates. In order to minimize the ohmic drop and to favour the diffusion of lithium through the bulk of the fibres (ca 6 micrometer of diameter), the reversible de-intercalation was evaluated at 25 mAg^{-1}.

3. RESULTS AND DISCUSSION.

3.1 Sample preparation and characterization. As the aim of the study was to investigate the influence of oxygenated group on the Li-ion intercalation performance, the surface of untreated commercial carbon cloth, referred to as "as-received carbon cloth", was modified by nitric acid vapour treatment {Xia 2009 #139} [25]. This treatment can effectively increase the amount of oxygen on the surface of carbon materials. Most precisely, it introduces a variety of different oxygen-containing functional groups {Kundu 2008 #145} [26], such as phenol, ester, ether, carboxylic, aldehyde, carbonyl or pyrone, on the carbon surface. Most of these groups can be removed from the surface by thermal treatment at temperatures up to 800º C. However, the removal

of different groups takes place at different conditions namely the treatment temperature and atmosphere {Kundu 2008 #145} [26]. Consequently, a set of samples with a large variety of amounts and types of oxygen-containing functional groups can be prepared by combining these treatment parameters. The preparation conditions of the samples are summarized in Figure 1.

The obtained carbon cloth samples were studied by XPS. The survey spectra of as-received and oxidized carbon cloth are shown in Figure 1a. Carbon and oxygen were detected in all the samples. Additionally, small amount of Si was also detected in the as-received sample, as indicated by its characteristic Si 2p (at about 103.5 eV) and Si 2s (at about 155.5 eV) peaks. The peak positions indicate that the Si present in form of oxide. HNO_3 vapour treatment for 24 h led to the removal of the Si species (trace 2 in Figure 2a). However, Si appeared again after prolonged exposure to HNO_3 vapour, namely in sample O-72 and O-144 (trace 3 and 4 in Figure 2a). The presence of Si species could be related to the production process of the carbon cloth. The oxide form of Si does not have influence on the lithium intercalation. However, it influences the XP O 1s spectra of related samples therefore have to be taken into account when analyzing the oxygen-containing functional groups.

The XP O1s spectra of the carbon cloth samples are shown in Figure 2b. There is agreement in literature on the assignment of the peaks in O 1s spectra {Kundu 2008 #145} [26]. The contributions of oxygen doubly bound to carbon (C=O) and oxygen singly bound to carbon (C-O) appear at 531.6 eV and 533.2 eV, respectively. Obviously, the strong contribution at about 532 eV in the as-received carbon cloth sample cannot be fitted by C=O or C-O peaks. The resolved peak at that position can be assigned to oxygen bound to silicon, which is in agreement with the survey spectra.

The surface atomic concentration of the carbon cloth samples were calculated from XPS measurements (Table 1). As-received carbon cloth contains 4.6 % of oxygen on surface, among which 2.0% is related to silicon species and 2.6% to carbon including oxygen-containing functional groups. Treatment in hydrogen at 800°C led to the decrease of oxygen species, mainly the oxygen-containing functional groups. This decrease is believed to be insignificant for the electrochemical performance of the samples since the overall amount of oxygen is low in both the as-received and hydrogen treated samples. Treatment in HNO_3 vapour led to significant increase of surface oxygen groups, as can be seen from Table 1. With the increase of treatment time, the oxygen amount increased from 8.3 % (24 h) to 10.3 % (72 h) and further to 10.9 % (144 h) after subtracting the contribution of silicon oxide.

Our previous studies showed the controlled removal of oxygen-containing functional groups on carbon surface by thermal treatment (25shankha JPCC 2008; W. Xia, X. Yin, S. Kundu, M. Sanchez, A. Birkner, C. Wöll, M. Muhler carbon 2011, 49, 299-305). The oxidized carbon cloth O-24 was treated at different temperature in helium or in hydrogen, and the XP spectra of the obtained samples were shown in Figure 3. It can be seen that the thermal treatment led to significant decrease of oxygen species on carbon cloth. Moreover, treatment in hydrogen at high temperatures (600°C and 800°C) led to the exposure of silicon species, as indicated by the strong contribution at about 532 eV (trace 3 and 4 in Figure 3b). Moreover, the XPS studies disclosed a relative change of C=O and C-O species. Treatment in helium resulted in the gradual decrease of both contributions with increasing treatment temperatures. However, hydrogen as a reducing agent is more effective in removal C=O than C-O at 600°C, where C-O can be formed by reducing C=O. At even higher temperature of 800°C, mainly bridged oxygen atoms such as ether- and pyrone-type are stable.

Quantitative analysis by XPS studies confirmed the significant decrease of oxygen-containing functional groups after the thermal treatment in helium or hydrogen (Table 1). The amount of oxygen after subtracting the oxygen bound to silicon was determined to be 2.3 % and 1.5% after treatment at 800°C in helium and hydrogen, respectively. Lower amount of oxygen was always detected in hydrogen than in helium at the same treatment temperature obviously due to the reactive nature of hydrogen.

3.2 The irreversible specific charge. Before the oxidative treatment of the sample was performed and evaluated, the effect of the thermal treatment on as-received carbon cloth was evaluated. The table 2 summarizes the irreversible capacities, calculated as the difference between intercalation and de-intercalation charge from the first galvanostatic cycle at 100 mAg^{-1}, as well as the reversible capacities extracted from the fifth de-intercalation at 25 mAg^{-1}. In the case of as-received, the irreversible specific charge decreases from 15 to 13 $mAhg^{-1}$ after the thermal treatment in H_2 at 800ºC. The surface oxygen concentration also decreases from 2.6 to 1.9 % which seems to indicate that the irreversibility increase with increased surface oxygen concentration.

A better visualization of the irreversible processes can be achieved by plotting the differential curves during the first negative-going sweep. The plateaus of the transient potential – time are transformed into peaks, as the inverse of the slope is plotted, which facilitate the localization of the potentials at which a reaction is taking place. The inset in Figure 4 shows the differential curves recorded at 100 mAg^{-1} for as-received carbon cloth before and after treatment in H_2 at 800º C. The differential curves shown in Figure 4 enable identifying two cathodic peaks at ca 0.8 V and at ca 0.5 V in both samples. According to literature {Chung 2000 #256}{Ng 2009 #138}{Jeong 2001 #41}[27-29], the reaction taking place at higher potential is attributed to the solid electrolyte interface

(SEI) formation, whereas the peak at lower potentials could be assigned to the exfoliation reaction. The latter process occurs when a poor SEI film is formed, which allows the solvated lithium to diffuse through the film into the graphene layers. Then, the solvent that solvates the lithium is reduced inside the bulk of the material which leads to damages in both material and SEI film. Therefore, a good SEI film needs to be formed, thick enough to prevent the diffusion of solvated lithium but spending as less charge as possible. In the case of as-received carbon cloth, a high efficiency of 98 % was already found in the second cycle in both samples, before and after the thermal treatment, which means that SEI film is not destroyed during the first cycle. Therefore, the contribution of exfoliation in the irreversible specific charge must be small. The reason is likely related to the nature of the material. Carbon cloth is synthesized by carbonizing an organic polymer, in our case, at moderate low temperature. However, high temperatures are required to obtain highly ordered and crystalline structure. As the crystallinity degree is not high in our carbon cloth, a lower impact of the exfoliation than graphite is expected. In order to support this thesis, we attempted to increase the exfoliation by using a 1:1 (volume) mixture of propylene carbonate (PC) and dimethyl carbonate (DMC) for as-received carbon cloth treated in H_2 at 800º C. It is well known that graphitic materials exfoliate strongly when propylene carbonate (PC) is mixed in the electrolyte {DEY 1970 #258}{Xu 2004 #268}{Zhang 2001 #269} [30-32]. However, the differential curves obtained in EC:DMC and PC:DMC, Figure 4, follow similar behaviours, not showing the large expected increase of exfoliation. Moreover, the irreversible specific charge shown in Table 2 increases only from 13 $mAhg^{-1}$ to 15 $mAhg^{-1}$ for EC:DMC and PC:DMC, respectively. It can be concluded that the exfoliation takes also place on carbon cloth but it has a lower impact than other graphic materials.

A noteworthy increase of irreversibility was observed when as-received carbon cloth was oxidized during 24 hours (table 2), as the initial value of 15 $mAhg^{-1}$ increases more than 100 %. The concentration of oxygenated groups can be raised by prolonging the time of the oxidative process. The irreversible specific charge increases from 34 $mAhg^{-1}$, to 45 $mAhg^{-1}$ and 50 $mAhg^{-1}$, as the time of the oxidative process is prolonged from 24 hours, to 72 hours and 144 hours, respectively. It must be noted that the open circuit potential also increase upon increasing amount of oxygenated groups. An open circuit of ca 1 V is found in as-received, jumping to values above 3 V after the oxidative treatment. The surface functionalities contribute to the irreversible specific charge during the first cycle. The increase of irreversible specific charge could be strictly attributed to the surface functionalities reduction which takes place above 1.3 V. The contribution of the region above 1.3 V in the total irreversible specific charge was calculated as the difference of the charge consumed in this region during the first cycle, irreversible plus reversible, and the second cycle, only reversible. As can be seen in Table 3, the irreversible specific charge in this region increases upon increasing amount of oxygenated groups. In order to asses the influence of oxygenated groups on electrolyte decomposition, the contribution of the oxygenated group region was subtracted from the total irreversible specific charge (Table 3). The amount of oxygenated groups influence on electrolyte decomposition since a clear increase of the irreversible specific charge consumed below 1.3 V is observed upon increasing surface oxygen concentration. The effect of surface functionalities on the electrolyte stability can be also seen in the differential plot, Figure 5. In contrast to as-received carbon cloth, only one peak is seen in oxidized samples. Although the peak shifts and sharpens upon prolonging oxidative time, the main feature is the absence of exfoliation after oxidative treatment regardless the time of oxidation.

The O-24h carbon cloth was subjected to post thermal treatments in H_2 or in He at different temperatures in order to remove oxygen from the surface. As can be seen in Table 2, the irreversibility decreases with increased temperature of the post thermal treatment. The values vary more gradually in the case of helium, which is likely due to the fact that the ratio between oxygenated groups remains roughly constant. On the contrary, the ratio between oxygenated groups with single and double bonds changes drastically for thermal treatments in hydrogen which may leads to slight deviation in the trend. Therefore, the results obtained in this series of samples confirm the previous trend: the irreversible charge loss increases upon increasing amount of oxygenated groups.

The open circuit potential was seen to decrease as the oxygen was removed from the surface. The Table 3 shows the contribution in the irreversible charge of the region above 1.3 V and the region below 1.3 V. The values increase upon increasing amount of oxygenated groups in both regions which points out that surface oxygen not only increases the irreversible specific charge due to the irreversible reduction of some groups, but also increases the charge consumed during the electrolyte decomposition.

The differential curves of O-24h and O-24h after thermal treatment in H2 and in He are shown in Figure 6.a and 6.b, respectively. The inset in each figure represent the transient in the entire range from 3 V to 0.01 V, which has been enlarged to facilitate the visualization of the main features that take place below 1.5 V. The shifting of the peaks over different treatments reveals that the electrolyte decomposition is strongly dependent on the surface functionalities. Our attention has been attracted to the presence of either one or two cathodic peaks. As discussed above, two peaks are observed in as-received samples, whereas only one peak appears after oxidative treatment. Still only one peak is observed in O-24h after treatment at 300ºC in either atmosphere, however two peaks are seen after treatment at 600ºC and 800ºC in H_2 and 800ºC in He. This means that there is

a limit value of surface oxygen concentration on carbon cloth above which only one peak during the electrolyte decomposition occurs. This limit is around 4 % of surface oxygen concentration, since O-24h-600He containing 4.3 % has only one and O-24h-600H_2 with 2.6 % shows two cathodic peaks of oxygen on surface.

3.3 The reversible specific charge. The reversible specific charge values, which are summarized in Table 2, were calculated from the fifth de-intercalation cycle at 25 mAg^{-1}. No changes were found for as-received carbon cloth before and after treatment in H_2 at 800º C. However, a progressive increment of the reversible specific charge was seen as the amount of oxygenated groups was increased. The values of 142 $mAhg^{-1}$, 155 $mAhg^{-1}$, 158 $mAhg^{-1}$ and 162 $mAhg^{-1}$ were obtained in as-received, O-24h, O-72h and O-144h samples, respectively. Following the same dependence, the reversible specific charge decreases as the oxygenated groups were gradually removed from the surface of the O-24h carbon cloth by thermal treatment. At the same temperature, the values recorded in samples treated in helium, 155 mAh g^{-1}, 150 mAh g^{-1} and 148 mAh g^{-1}, are higher than those in hydrogen, 152 mAh g^{-1}, 149 mAh g^{-1} and 147 mAh g^{-1}, because the latter atmosphere is more reductive and removes a larger number of oxygenated groups, Table 1. The ratio between oxygenated groups with single and double bonds seems not to influence on the reversible specific charge. This is due to the fact that the reversible intercalation takes mainly place in the bulk of the materials, whereas the reduction of the electrolyte that is strongly influenced by the reactivity of the surface occurs on the surface.

In order to determine the potential at which the improvement in the reversible de-intercalation takes place, the differential curves during the fifth de-intercalation were plotted. The Fig. 7 shows the transients of as-received, O-24h, O-72h and O-144h carbon cloth. The insert in the figure represents the entire range of potentials, 0.01 – 3.00 V. The

main features appear above 0.5 V, thus a magnification of that region is also shown. Whereas the peak due to the de-intercalation from the graphene layers at ca 0.1 V remains approximately constant for the four samples, a new peak appears at ca 0.9V after the oxidation of the carbon cloth. In addition, the intensity of the transients raises its value at potentials above 1.3 V as the time of the oxidative treatment is prolonged. Oxygen functional groups have been proposed to be responsible of reversible anodic peaks at ca. 2.5 V {Gao 2000 #74}{Lee 2010 #263} [33-34]. In our case, the presence of many different oxygenated groups leads to the overlapping of several peaks at potentials above 1.3 V. The source of the de-intercalation peak at 0.9 V is more uncertain. One plausible explanation is based on the carbon hybridization. As proven by Dahn et al {ZHENG 1996 #271} [35], the lithium intercalated into carbon with sp^3 hybridization, instead of sp^2, bounded to hydrogen de-intercalates at ca 1 V. Consequently, the appearance of the peak at 0.9 V might be due to the intercalation into oxygenated carbons with sp^3 hybridization. The dependence of these two features in the transients on the presence of oxygenated groups was confirmed by thermal treatment, Fig 8. As the oxygenated groups are removed from the surface by rising the temperature of the treatment, the peak at 0.9 V disappears and the intensity of the transient at above 1.3 V decreases gradually. This trend is seen in the series of samples prepared in both helium and hydrogen atmospheres.

The Table 4 enables a quantitative evaluation of the de-intercalation from these two regions. The ranges of 0.6 V – 1.2 V and 1.2 V – 3.0 V, which are referred to as region 1 and region 2 respectively, were chosen to evaluate the new features of the transients. The values in both regions decrease for as-received after thermal treatment and increase after oxidative treatment, continuing rising upon prolonging oxidative time. It indicates that the increase of reversible specific charge in these two regions, specially the region 2, is due to a larger amount of the surface functional groups. The values obtained

for 24h oxidised carbon cloth subjected to thermal treatments are consistant with the previous trend, decreasing specific charge in both regions were observed upon decreasing amount of oxygen concentration. The reversible capacities in both regions were slightly lower in H_2 than He treatment at the same temperature because the surface oxygen concentration was also lower in H_2, as discussed above.

4. CONCLUSIONS.

The amount of oxygenated groups that were introduced on the surface of carbon cloth by gas-phase nitric acid treatment was increased upon prolonging the treatment time, as indicated by the XPS measurements. The concentration of surface oxygen of the oxidized carbon cloth was seen to decrease by increasing the temperature of thermal treatment in both helium and hydrogen. The latter atmosphere was able to remove a larger amount of surface functionalities than He at the same temperature.

The irreversible specific charge was found to increase upon increasing amount of surface functionalities. Two cathodic peaks were observed in the first negative-going sweep in as-received carbon cloth and for the samples with concentration of surface oxygen lower than 4 %. However, only peak appeared in the samples with concentration of surface oxygen larger than 4 %.

An increase in surface functionalities also leads to an increase in the reversible specific charge. Two regions were primarily affected after introducing surface functionalities, a reversible anodic process appeared at ca 0.9 V and several overlapped ones at above 1.3 V. The peaks decreased in intensity as the oxygenated groups were removed from the surface using a thermal treatment in H_2 and He.

ACKNOWLEDGMENT.

Financial support by the BMBF in the framework of the project “Elektrochemie und Mobilität – Kompetenzverbund Nord” is gratefully acknowledged.

FIGURE CAPTIONS.

Figure 1. Schematic representation of the samples preparation.

Figure 2. XP survey (a) and O 1s (b) spectra. (1) as-received carbon cloth, and after treatment in HNO3 vapor at 200°C for (2) 24 h, (3) 72 h and (4) 144 h.

Figure 3. XP O 1s spectra of carbon cloth samples oxidized by HNO3 vapor at 200°C for 24 h (1) and treated at 300°C (2), 600°C (3) and 800°C (4) in helium (a) and hydrogen (b). The O1s peaks were normalized to the intensity of corresponding C 1s peaks.

Figure 4. Differential capacity versus potential obtained from the first galvanostatic intercalation at 100 mA g^{-1} for as-received carbon cloth, as-received after treatment in hydrogen at 800º C in 1:1 EC:DMC, and as-received after treatment in hydrogen at 800º C [b] in 1:1 PC:DMC solution.

Figure 5. Differential capacity versus potential obtained from the first galvanostatic intercalation at 100 mA g^{-1} for carbon cloth samples oxidized by HNO3 vapor at 200°C for 24 h (O-24h), 72 h (O-72h) and 144 h (O-144h).

Figure 6. Differential capacity versus potential obtained from the first galvanostatic intercalation at 100 mA g^{-1} for samples treated in helium (A) and hydrogen (B). The inset represents the entire range of potential, from 3 V to 0 V, which has been magnified to provide a better visualization of the features.

Figure 7. Differential capacity versus potential obtained from the fifth galvanostatic de-intercalation at 25 mA g^{-1} for as-received carbon cloth (As-rec) and carbon cloth samples oxidized by HNO3 vapor at 200°C for 24 h (O-24h), 72 h (O-72h) and 144 h (O-144h) The inset represents the entire range of potential, from 3 V to 0 V, which has been magnified to provide a better visualization of the features.

Figure 8. Differential capacity versus potential obtained from the fifth galvanostatic de-intercalation at 25 mA g^{-1} for carbon cloth samples treated in helium (A) and (B) hydrogen. The inset represents the entire range of potential, from 3 V to 0 V, which has been magnified to provide a better visualization of the features.

Figure1.

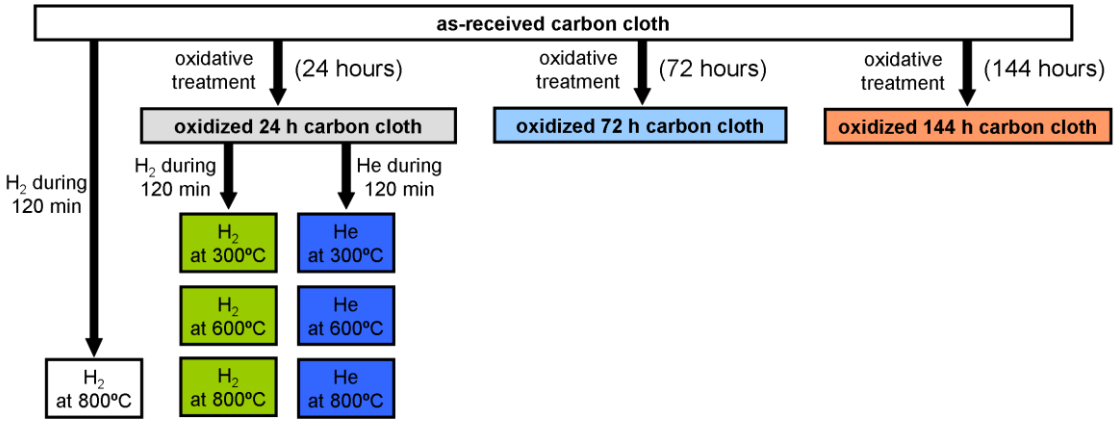
as-received carbon cloth
oxidative treatment
(24 hours)
oxidative treatment
(72 hours)
oxidative treatment
(144 hours)
oxidized 24 h carbon cloth
oxidized 72 h carbon cloth
oxidized 144 h carbon cloth
H2 during 120 min
H2 during 120 min
He during 120 min
H2 at 300ºC
He at 300ºC
H2 at 600ºC
He at 600ºC
H2 at 800ºC
H2 at 800ºC
He at 800ºC

Figure 2.

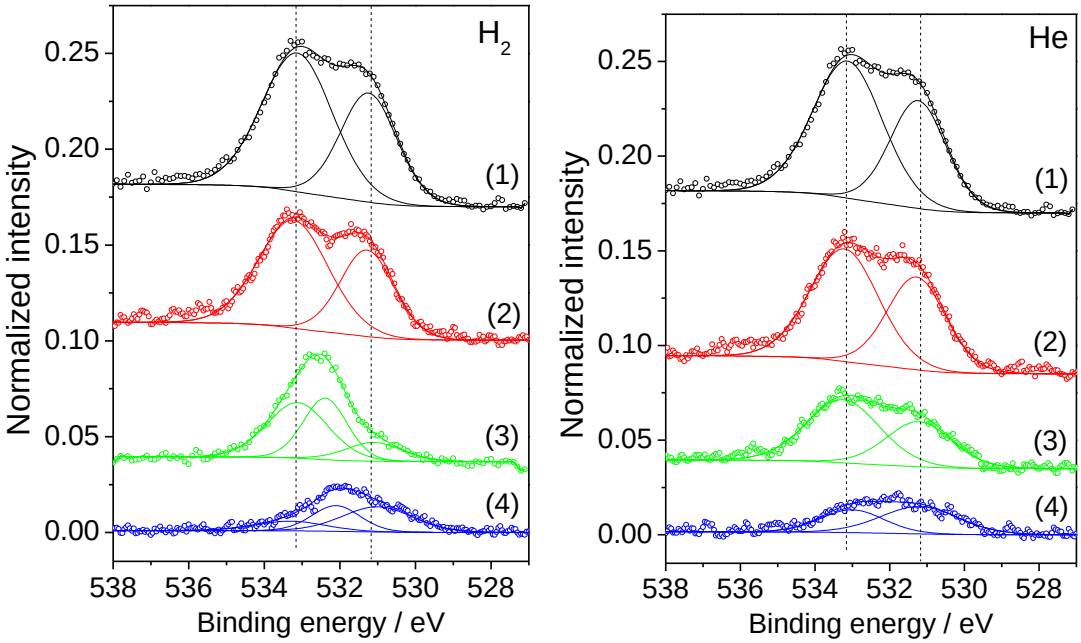
H2
He
(1)
(2)
(3)
(4)
Normalized intensity
0.25
0.20
0.15
0.10
0.05
0.00
538
536
534
532
530
528
Binding energy / eV

Figure 3.

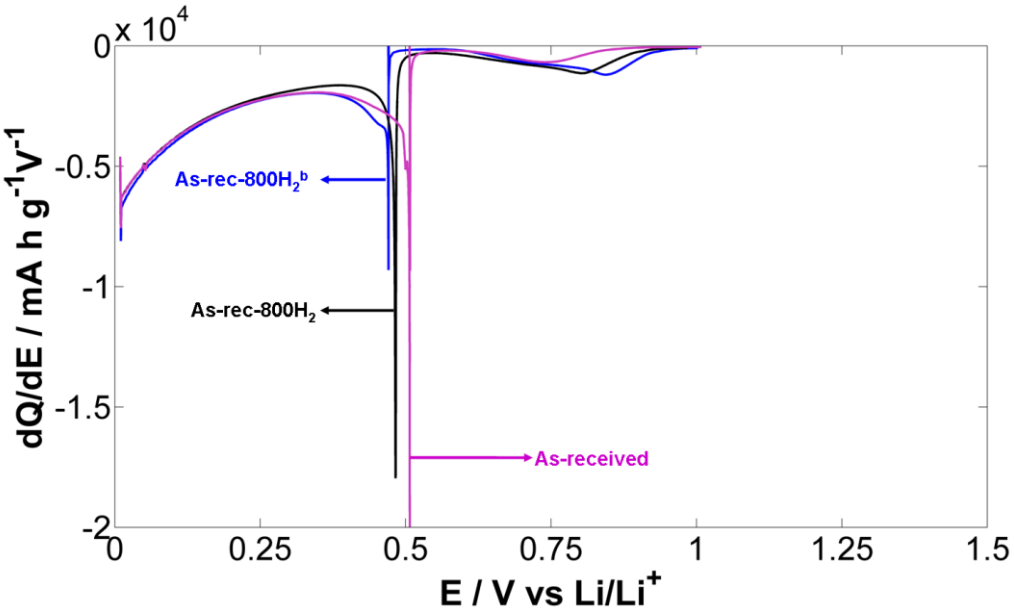
x 10^4
0
-0.5
-1
-1.5
-2
dQ/dE / mA h g^-1 V^-1
As-rec-800H2^b
As-rec-800H2
As-received
0
0.25
0.5
0.75
1
1.25
1.5
E / V vs Li/Li+

Figure 4.

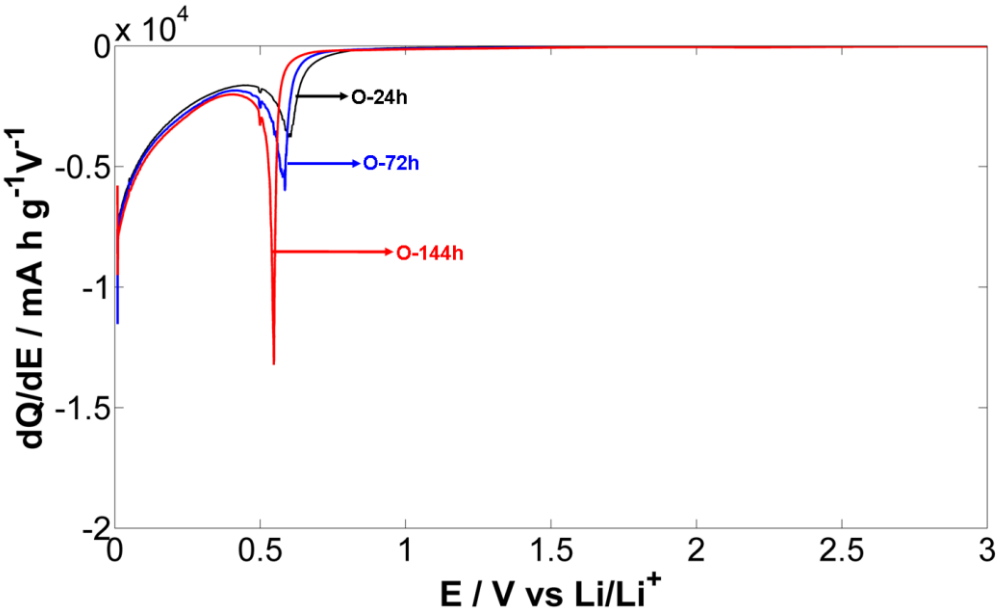
x 10^4
0
-0.5
-1
-1.5
-2
0
0.5
1
1.5
2
2.5
3
dQ/dE / mA h g^-1V^-1
E / V vs Li/Li+
O-24h
O-72h
O-144h

Figure 6.

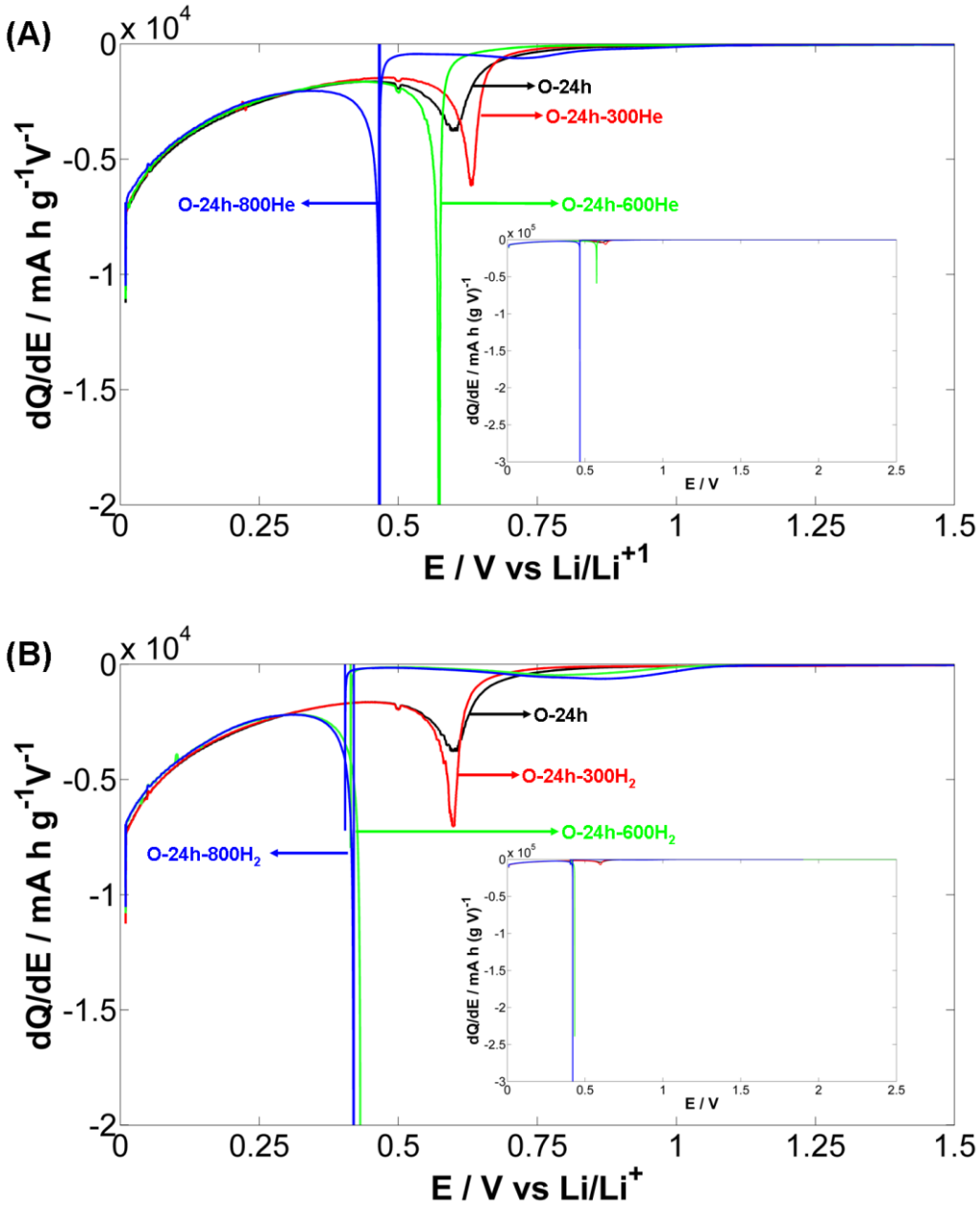
(A)
x 10^4
dQ/dE / mA h g^-1 V^-1
E / V vs Li/Li^+1
O-24h
O-24h-300He
O-24h-600He
O-24h-800He
x 10^5
dQ/dE / mA h (g V)^-1
E / V
(B)
x 10^4
dQ/dE / mA h g^-1 V^-1
E / V vs Li/Li^+
O-24h
O-24h-300H2
O-24h-600H2
O-24h-800H2
x 10^5
dQ/dE / mA h (g V)^-1
E / V

Figure 7.

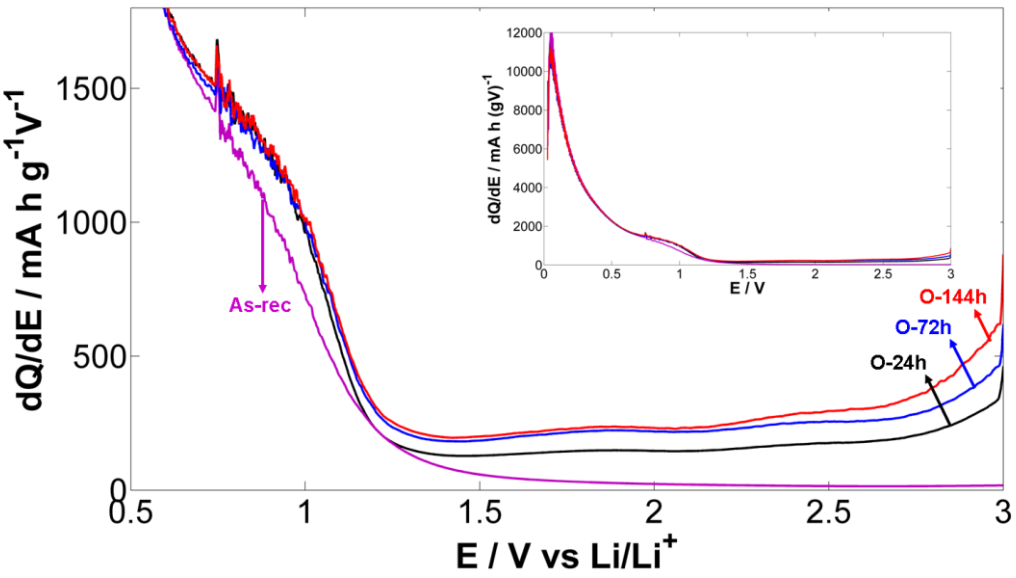

Figure 8.

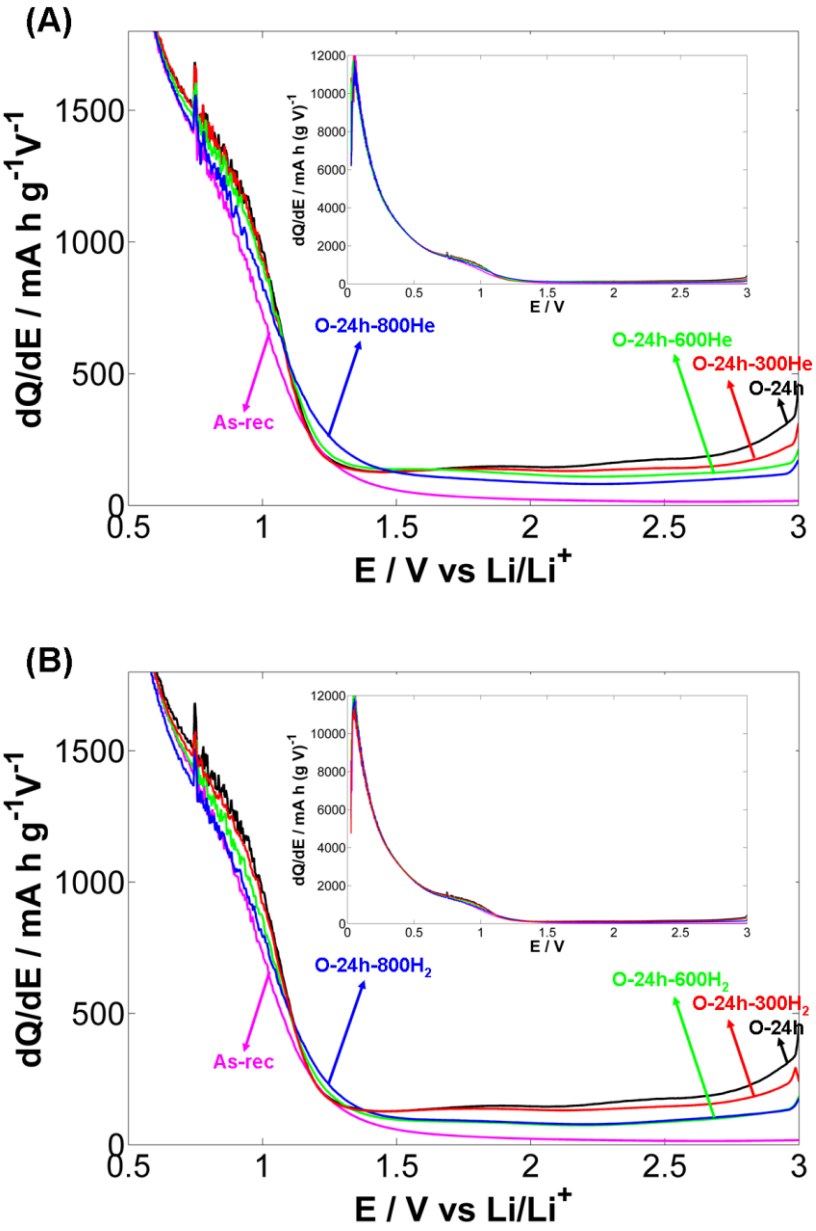
(A)
dQ/dE / mA h g-1V-1
E / V vs Li/Li+
dQ/dE / mA h (g V)-1
E / V
As-rec
O-24h-800He
O-24h-600He
O-24h-300He
O-24h
(B)
dQ/dE / mA h g-1V-1
E / V vs Li/Li+
dQ/dE / mA h (g V)-1
E / V
As-rec
O-24h-800H2
O-24h-600H2
O-24h-300H2
O-24h

TABLES.

Table 1. Surface atomic concentrations of oxygen and carbon derived from XPS measurements. [a] Silicon oxide was detected as impurities present in the as-received carbon cloth and carbon cloth after certain treatment. The oxygen in silicon oxide was excluded during calculation.

Table 2. The irreversible capacity of the first cycle and the reversible capacity of the fifth de-intercalation for different samples. [b] 1:1 Mixture of PC:DMC instead of 1:1 EC:DMC

Table 3. The charge spent during the first intercalation at 100 mAg^{-1} divided into two regions: oxygenated groups reduction (above 1.3 V), and SEI formation plus exfoliation, and charge spent during the fifth deintercalation at 25 mAg^{-1} divided into other two regions: between 0.6 V and 1.2 V, and above 1.2 V. [b] 1:1 Mixture of PC:DMC instead of 1:1 EC:DMC

Table 1.

Sample and treatment conditions		O% in O-groups	O% in SiO2	C%
as-received	Untreated	2.6	2.0	95.4
	H2@800ºC	1.9	1.9	96.2
HNO_3 vapor 200°C	O-24h	8.3	0	91.7
	O-72h	10.0 [a]	2.6	87.4
	O-144h	10.4 [a]	4.2	85.4
O-24h, in helium	300°C	6.9	0	93.1
	600°C	4.3	0	95.7
	800°C	2.2	0	97.7
O-24h, in hydrogen	300°C	6.2	0	93.8
	600°C	2.6 [a]	1.6	95.8
	800°C	1.5 [a]	0.7	97.8

Table 2.

Sample and treatment conditions		Irrevers Cap ($mAhg^{-1}$)	Revers Cap ($mAhg^{-1}$)
as-received	Untreated	15	142
	H2@800ºC	13	142
	H2@800ºC[b]	15	140
HNO_3 vapor 200°C	O-24h	34	155
	O-72h	45	158
	O-144h	50	162
O-24h, treated in helium	300°C	29	155
	600°C	27	150
	800°C	25	148
O-24h, treated in hydrogen	300°C	31	152
	600°C	27	149
	800°C	28	147

Table 3.

Sample and treatment conditions		Surface Oxygen Concen (%)	Irreversible capacity ($mAhg^{-1}$)		Reversible capacity ($mAhg^{-1}$)	
			>1.3 V	SEI+Exf	0.6-1.2V	>1.2V
as-received	Untreated	2.6	0	15	24	3
	H2@800º C	1.9	0	13	23	2
	H2@800º C[b]	1.9	0	15	24	2
HNO_3 vapor 200°C	O-24h	8.3	3	31	28	13
	O-72h	10.0	5	40	28	18
	O-144h	10.4	6	44	29	21
O-24h helium	300°C	6.9	2	27	28	11
	600°C	4.3	1	26	28	9
	800°C	2.2	1	24	27	9
O-24h hydrogen	300°C	6.2	2	29	28	11
	600°C	2.6	1	28	26	8
	800°C	1.5	1	29	25	8

REFERENCES.

(1) Tarascon, J. M.; Armand, M. *Nature* **2001**, *15*, 359.

(2) Tarascon, J. M. *Philos. T. R. Soc. A* **2010**, *368*, 3227.

(3) Bruce, P. G.; Scrosati, B.; Tarascon, J.-M. *Angew. Chem. Int. Ed.* **2008**, *47*, 2930.

(4) Fong, R.; Von Sacken, U.; Dahn, J. R. *J. Electrochem. Soc.* **1990**, *137* , 2009.

(5) Zheng, T.; Liu, Y. H.; Fuller, E. W.; Tseng, S.; Vonsacken, U.; Dahn, J. R. *J. Electrochem. Soc.* **1995**, *142* (8), 2581–2590.

(6) Dahn, J. R.; Zheng, T.; Liu, Y. H.; Xue, J. S. *Science* **1995**, *270*, 590.

(7) Winter, M.; Besenhard, J. O.; Spahr, M. E.; Novak, P. *Adv. Mater.* **1998**, *10*, 725.

(8) Aurbach, D.; Eineli, Y.; Chusid, O.; Carmeli, Y.; Babai, M.; Yamin, H. *J. Electrochem. Soc.* **1994**, *141*, 603.

(9) Aurbach, D.; Eineli, Y.; Markovsky, B.; Zaban, A.; Luski, S.; Carmeli, Y.; Yamin, H. *J. Electrochem. Soc.* **1995**, *142*, 2882.

(10) Jeong, S. K.; Inaba, M.; Mogi, R.; Iriyama, Y.; Abe, T.; Ogumi, Z. *Langmuir* **2001**, *17*, 8281.

(11) Aurbach, D.; Markovsky, B.; Weissman, I.; Levi, E.; Ein-Eli, Y. *Electrochim. Acta* **1999**, *45*, 67.

(12) Novak, P.; Goers, D.; Hardwick, L.; Holzapfel, M.; Scheifele, W.; Ufhiel, J.; Wursig, A. *J. Power Sources* **2005**, *146*, 15.

(13) Larcher, D.; Mudalige, C.; Gharghouri, M.; Dahn, J. R. *Electrochim. Acta* **1999**, *44*, 4069.

(14) Spahr, M. E.; Wilhelm, H.; Joho, F.; Panitz, J. C.; Wambach, J.; Novak, P.; Dupont-Pavlovsky, N. *J. Electrochem. Soc.* **2002**, *149*, A960.

(15) Spahr, M. E.; Wilhelm, H.; Palladino, T.; Dupont-Pavlovsky, N.; Goers, D.; Joho, F.; Novak, P. *J. Power Sources* **2003**, *119*, 543.

(16) Beguin, F.; Chevallier, F.; Vix-Guterl, C.; Saadallah, S.; Bertagna, V.; Rouzaud, J. N.; Frackowiak, E. *Carbon* **2005**, *43*, 2160.

(17) Gao, B.; Kleinhammes, A.; Tang, X. P.; Bower, C.; Fleming, L.; Wu, Y.; Zhou, O. *Chem. Phys. Lett.* **1999**, *307*, 153.

(18) Chen, J.; Minett, A. I.; Liu, Y.; Lynam, C.; Sherrell, P.; Wang, C.; Wallace, G. G. *Adv. Mater.* **2008**, *20*, 566.

(19) Landi, B. J.; Ganter, M. J.; Schauerman, C. M.; Cress, C. D.; Raffaelle, R. P. *J. Phys. Chem. C* **2008**, *112*, 7509.

(20) Shimoda, H.; Gao, B.; Tang, X. P.; Kleinhammes, A.; Fleming, L.; Wu, Y.; Zhou, O. *Phys. Rev. Lett.* **2002**, *88*, 015502-1.

(21) Ajayan, P. M.; Ebbesen, T. W.; Ichihashi, T.; IIjima, S.; Tanigaki, K.; Hiura, H. *Nature* **1993**, *362*, 522.

(22) Klein, K. L.; Melechko, A. V.; McKnight, T. E.; Retterer, S. T.; Rack, P. D.; Fowlkes, J. D.; Joy, D. C.; Simpson, M. L. *J. Appl. Phys.* **2008**, *103*, 061301.

(23) Bitter, J. H. *J. Mater. Chem.* **2010**, *20*, 7312.

(24) Beguin, F.; Chevallier, F.; Vix, C.; Saadallah, S.; Rouzaud, J. N.; Frackowiak, E. *J. Phys. Chem. Solid* **2004**, *65*, 211.

(25) Xia, W.; Jin, C.; Kundu, S.; Muhler, M. *Carbon* **2009**, *47*, 919.

(26) Kundu, S.; Wang, Y.; Xia, W.; Muhler, M. *J. Phys. Chem. C* **2008**, *112*, 16869.

(27) Chung, G. C.; Kim, H. J.; Yu, S. I.; Jun, S. H.; Choi, J. W.; Kim, M. H. *J. Electrochem. Soc.* **2000**, *147*, 4391.

(28) Ng, S.; Vix-Guterl, C.; Bernardo, P.; Tran, N.; Ufheil, J.; Buqa, H.; Dentzer, J.; Gadiou, R.; Spahr, M.; Goers, D.; Novák, P. *Carbon* **2009**, *47*, 705.

(29) Jeong, S.-K.; Inaba, M.; Abe, T.; Ogumi, Z. *J. Electrochem. Soc.* **2001**, *148*, A989.

(30) Dey, A. N.; Sullivan, B. P. *J. Electrochem. Soc.* **1970**, *117*, 222.

(31) Xu, K. *Chem. Rev.* **2004**, *104*, 4303.

(32) Zhang, X. R.; Kostecki, R.; Richardson, T. J.; Pugh, J. K.; Ross, P. N. *J. Electrochem. Soc.* **2001**, *148*, A1341.

(33) Gao, B.; Bower, C.; Lorentzen, J. D.; Fleming, L.; Kleinhammes, A.; Tang, X. P. *Chem. Phys. Lett.* **2000**, *327*, 69.

(34) Lee, S. W.; Yabuuchi, N.; Gallant, B. M.; Chen, S.; Kim, B. S.; Hammond, P. T.; Shao-Horn, Y. *Nat. Nanotechnol.* **2010**, *5*, 531.

(35) Zheng, T.; McKinnon, W. R.; Dahn, J. R. *J. Electrochem. Soc.* **1996**, *143*, 2137.